Growth of ultrathin rare-earth films studied by *in situ* x-ray diffraction

C. L. Nicklin, M. J. Everard, and C. Norris
Department of Physics and Astronomy, University of Leicester, University Road, Leicester LE1 7RH, United Kingdom

S. L. Bennett
CLRC Daresbury Laboratory, Keckwick Lane, Warrington WA4 4AD, United Kingdom
(Received 15 March 2004; revised manuscript received 11 August 2004; published 13 December 2004)

We present *in-situ* x-ray scattering measurements performed during the growth of two rare-earth metals, gadolinium and samarium, onto molybdenum (110) single crystals. The results have been interpreted using a diffusive growth model to determine the degree of interlayer mass transport in the initial stages of deposition. Both elements are shown to grow generally in a layerwise manner but with significant roughness after the initial layer is complete. A raised substrate temperature modifies the growth; the best Gd single layer is produced at a temperature of 140 °C when deposited at a rate of 0.067 monolayers/min while for Sm the growth becomes increasingly islanded at higher temperatures. The presence of oxygen at the surface encourages layer-by-layer growth for both Gd and Sm, although a significant proportion of the atoms are in upper layers before the lower ones are complete. The mechanism for improved layerwise growth is oxide formation at the interface, producing a large amount of small islands that encourage interlayer mass transport. The growth of Sm on Mo(110) is generally more rough than Gd on Mo(110) due to the dynamic size change associated with the coordination induced valence transition for the Sm atoms.

DOI: 10.1103/PhysRevB.70.235413 PACS number(s): 68.35.Ct, 68.55.Jk

I. INTRODUCTION

The growth of rare earth (RE) metals onto a variety of substrates has continued to attract much attention. The interest arises from the unique properties that are displayed as a consequence of the correlations between the electrons in the partially filled and highly localized $4f$ orbitals and the extended $5d6s$ valence states. This can lead to interesting magnetic behavior in RE elements such as gadolinium (Gd), which has seven unpaired $4f$ electrons. In its bulk state Gd exhibits a single ferromagnetic phase with a Curie transition temperature (T_c) of 293 K, the highest to be found in the series. At the surface of Gd, however, it has been shown that T_c is approximately 20 K higher than the bulk value.[1,2] Gd has also been shown to couple antiferromagnetically to an Fe(001) surface,[3] encouraging further studies of thin Gd films or multilayers for use in magnetic devices. The valence state of the RE atom is another property that can be varied, as the energy of the divalent and trivalent configurations is sufficiently close that fluctuations can occur between them. Such intermediate or mixed valence behavior can be caused by thermal effects[4] or a change in the chemical environment of the RE atom in materials such as TmSe.[5] The difference in energy as a result of the reduced coordination of the RE atom at the surface of a sample can also stabilize a different valence to that of the bulk material. This is particularly noteworthy in samarium (Sm), where the difference between the $4f^6(5d6s)^2$ and the $4f^5(5d6s)^3$ states is only $\sim$6 kcal/mol, implying the complete $2d$ surface of samarium will be divalent whilst the bulk is trivalent.[6] This produces interesting epitaxial effects, as incomplete mutual electron screening means that the diameter of the divalent atom is significantly larger than a trivalent one. This leads the surface of a bulk Sm single crystal to show a (11×11) reconstruction with significant corrugation of the topmost divalent layer.[7] The potential of using such fluctuations in devices has been demonstrated by, for example, the production of a three-dimensional optical memory that uses the valence of Sm to represent a bit of information and lasers to switch the state.[8]

Ultrathin layers of RE metals and alloys prepared by controlled deposition in ultrahigh vacuum present a valuable opportunity to study the effects of strong atomiclike correlations perturbed by the presence of a nonlocalized conduction band. Many different substrates have been used including semiconductors such as silicon, germanium, or gallium arsenide, where significant alloy formation occurs. Surface x-ray diffraction (SXRD) has been used to establish the structure of an ultrathin layer of Er on Si(111), indicating that the Er atoms sit below a silicon bilayer on top of a bulk terminated crystal.[9,10] The structure has been confirmed by medium energy ion scattering (MEIS) by Spence *et al.*,[11] who present similar results for Ho on Si(111), Dy on Si(111),[12] and Dy on Ge(111).[13] In all cases, for deposition of one equivalent monolayer, the RE atoms are found to reside below a bilayer of the semiconductor material.

Equally important are studies of RE metals grown on non-alloying substrates where two-dimensional layer growth is encouraged.[14–16] The (110) surface of the body-centered-cubic refractory metals, molybdenum and tungsten, yield a morphology with low corrugation and a resistance to intermixing. Kolaczkiewicz and Bauer[17] and Stenborg *et al.*[18,19] used several laboratory-based techniques to establish the fundamental growth mode and submonolayer structures for Gd and Sm deposited on tungsten and molybdenum. Both materials show a series of $(n\times 2)$ structures prior to hexagonal or pseudohexagonal monolayers, similar to the RE(0001) surface. Subsequent deposition follows the layer-by-layer growth mode, although with increasing roughness. Sa-

marium in particular shows poor layerwise growth due to the changing valence with coverage.

Previous *in situ* surface diffraction results have been reported for room-temperature growth of Gd on Mo(110),[20] Sm on Mo(110),[21] and Ho on Mo(110).[22] In this case the period of the oscillations was observed to change depending on the perpendicular momentum transfer vector (ℓ) at which the growth was monitored. This effect is due to the changing sensitivity to particular layer heights at different ℓ values and the way the scattering from the surface layers interfere with the underlying substrate scattering. This variation is inherent to the model we present later.

Here, we report how the growth of two of the RE elements (Gd and Sm) on Mo(110) is affected by temperature or through preexposure to oxygen. Fits to the data are based on a three-level diffusive growth model that allows for a limited degree of bilayer formation and gives an indication of the degree of interlayer mass transport. Such quantitative information provides an important insight as to how the RE's grow on Mo(110) and how the dynamics of growth are affected by external parameters such as temperature or the presence of contaminants.

II. EXPERIMENT

The measurements were recorded on beamline 9.4 of the Synchrotron Radiation Source (SRS) at Daresbury Laboratory using the five-circle x-ray diffractometer. Radiation of wavelength 0.9 Å was selected from the 5-T wiggler using a channel cut Si(111) monochromator. The scattered x-ray intensity was recorded using a cooled germanium detector mounted behind two sets of four-jaw slits to define the angular resolution.

The sample was mounted inside an ultrahigh vacuum (UHV) chamber that was equipped with metal vapor sources, low-energy electron diffraction (LEED) optics, and a hemispherical electron energy analyzer for Auger electron spectroscopy (AES) measurements.[23] The Mo crystal was cut and electropolished to within 0.1° of the (110) surface. A clean sample was produced by extended heating at 1000 °C in an atmosphere of 1×10^{-8} mbar of oxygen followed by flashing to 1800 °C in vacuum until contamination levels were minimized. No oxygen or sulfur was detectable by AES and the carbon signal was always less than 4% of the main Mo (186 eV) Auger peak. The RE metals were deposited from a tantalum crucible in a Knudsen cell, surrounded by a water-cooled shroud. The base pressure of the chamber was 8×10^{-11} mbar and no pressure rise was detected during evaporation. Each growth curve was recorded after thorough cleaning of the Mo(110) surface, as described above. The crystal was allowed to stabilize for 60 min at the temperatures indicated before deposition began. The growth in oxygen was achieved by exposing the sample to the amount of gas specified, with the sample held at room temperature.

Three-level diffusive growth model

The layerwise growth of the RE material on top of bulk terminated Mo(110) can be modeled using kinematic scattering theory. At any point except the Bragg position, the total scattering amplitude from a single column of bulk terminated unit cells is given by

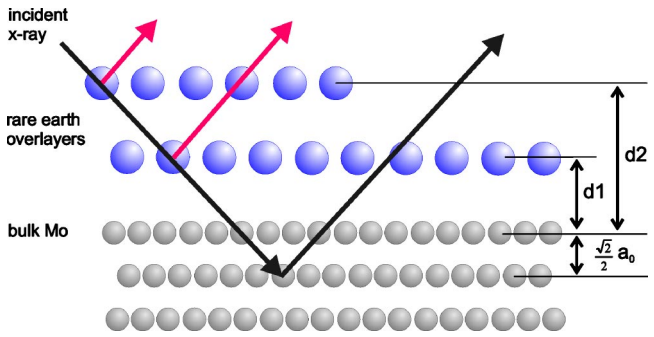

FIG. 1. (Color online) Structural model used in fitting the specular intensity as a function of deposition time. The heights of the adlayers (d_1,d_2) above the Mo(110) substrate can be determined.

$$F_{00\ell}^{bulk} = \frac{f^{\mathrm{Mo}}}{1-\exp[-\pi i\ell]}, \tag{1}$$

where f^{Mo} is the atomic scattering factor for Mo and ℓ is the perpendicular reciprocal lattice vector, determined from the substrate unit cell. The heterogeneous growth model is based on the separation of successive layers of material from the bulk terminated surface, as shown in Fig. 1. In our definition, the repeat distance perpendicular to the surface is $\sqrt{2}a_0$, where a_0 is the Mo lattice parameter (3.15 Å) and the first Bragg scattering points occurs at $\ell=2.0$. The total scattering amplitude in this case is given by the sum of the bulk scattering with the contribution from each individual layer:

$$F_{00\ell}^{total} = F_{00\ell}^{bulk} + \sum_n \theta_n f^{RE} \exp\left[\frac{2\pi i\ell}{\sqrt{2}a_0} d_n\right]. \tag{2}$$

Here n surface layers are included in the model where the atomic scattering factor for the adsorbate (either Gd or Sm) is given by f^{RE} and d_n is the height of the nth layer above the Mo surface. Each layer has a relative occupancy of θ_n, where $\theta=1$ corresponds to a complete unrelaxed Mo(110) plane (14.3×10^{18} atoms m^{-2}). The adlayers are assumed to form hexagonal close packed structures (consistent with the LEED results) at monolayer coverage, yielding an atomic density of 8.73×10^{18} atoms m^{-2} for Gd, which corresponds to a theoretical occupancy limit of $\theta=0.613$. Similarly, a trivalent Sm layer has a calculated occupancy limit of $\theta=0.617$.

The three-level diffusive growth model is an extension of a model previously used to fit x-ray scattering growth curves.[20,21] It incorporates simultaneous bilayer growth, under the conditions that the rate of growth (R) summed over all layers is constant and that layer $n+1$ does not have a higher occupancy than layer n. The model allows for the initial growth to follow a strictly layer-by-layer mode that is superseded by bilayer formation with exponentially increasing occupancy of the $n+1$ level. The additional features of the model are incorporated by an extra parameter per layer (s_n), which corresponds to the percentage occupancy of layer $n+1$ when layer n becomes fully occupied. The background

level was determined from a transverse scan around the deposition position prior to RE growth and the model assumes that this does not change during overlayer adsorption. A scale factor was found from the clean Mo(110) surface signal, to account for the experimental geometry. It should be noted that in some of the fits, the model is truncated in the second layer due to the breakdown of the model.

III. RESULTS AND DISCUSSION

Most of the x-ray results show how the intensity of specularly scattered x-ray varies during the deposition of the RE onto Mo(110) for different beam incidence angles. This corresponds to monitoring the growth at different positions along the (00ℓ) rod, yielding information about the morphology perpendicular to the substrate surface. Growth at $\ell = 1.0$ corresponds to the Mo(110) out of phase condition (also known as the anti-Bragg position), affording maximum sensitivity to the nucleation of islands with a perpendicular layer spacing equal to the bulk layer separation (2.23 Å). The other values of ℓ were calculated to be sensitive to the hard sphere separation of RE atoms in bridge sites of an unrelaxed Mo(110) surface. Adsorption at bridge sites was the model favored by Stenborg and Bauer.[24]

A. Room-temperature growth

1. Gd on Mo(110)

Gadolinium on molybdenum is an ideal system to study, since the elements do not form any known alloys and have very low mutual immiscibility. The controversy that surrounds the results reported for the magnetic properties of ultrathin Gd films arises from the specific microstructure of the films, such as the presence of defects and strain fields.[25–28] Here we report a structural study of Gd on Mo(110) and fits to the x-ray growth curves recorded at room temperature.

Initial experiments including AES, LEED, and work function change curves were performed to establish the submonolayer structures that occur for Gd on Mo(110). The work function curve, shown in Fig. 2, was measured using an ac retarding potential technique as described by Nathan and Hopkins.[29] It shows the characteristic features for an electropositive adsorbate, that is, an initial drop to a minimum (-2.29 eV) followed by a rise to a maximum due to the atomic smoothness at one monolayer coverage.

Subtle differences between the growth on W(110) and Mo(110) are revealed by the work function change curve. Using the Helmholtz equation

$$\Delta\phi = -300 \times 10^{-18} 4\pi np, \tag{3}$$

where the work function change $\Delta\phi$ is in eV and n is the concentration of adatoms per cm^2, the dipole moment (p) at the zero coverage limit is calculated to be 3.2 D (debye), which is lower than the value of 3.75 D when deposited on W(110). This implies a lower charge transfer on the Mo(110) surface, a trend that continues throughout the submonolayer region. The general shape of the work function curve can be understood in terms of the phase changes that occur. The

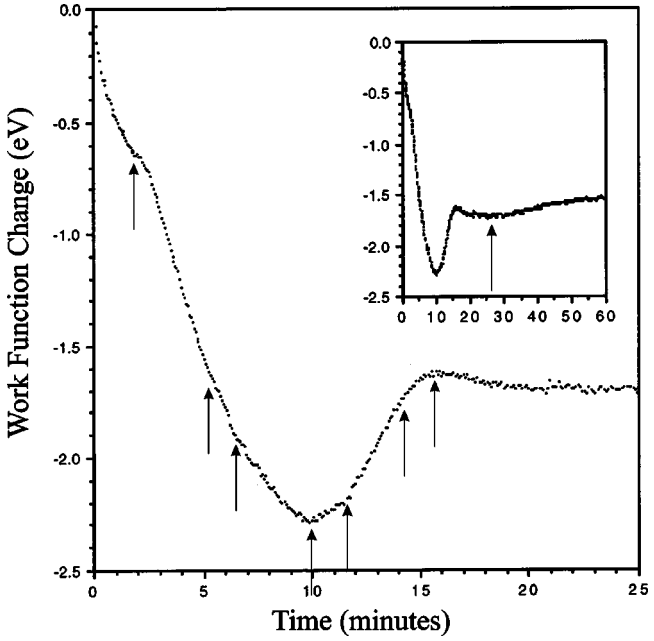

FIG. 2. Work function change as a function of Gd deposition time. Points discussed in the text are indicated by arrows. The inset shows the full curve up to three monolayers.

shoulder at 2.1 min is caused by the disappearance of the random overlayer gas with large dipole moments and the formation of ordered structures. A number of subtle breaks occur that are caused by the locking in of the different $n \times 2$ structures. At the minimum point the adatom density is large enough for the charge transfer to be reversed. A final break occurs shortly after the minimum, which signifies the point at which the adatom-adatom interactions dominate the adatom-substrate ones and the surface potential becomes isotropic. The rise to the maximum at one monolayer is caused by the gradual contraction of the overlayer to create a dense hexagonal structure. Beyond the monolayer, the shallow minimum indicates rough growth in the second layer, before the rise to a second layer completion point. These results therefore indicate a layerwise growth mode but with significant roughness occurring after the completion of the first monolayer.

The sequence of structures identified from LEED patterns recorded at different submonolayer points is summarized in the phase diagram shown in Fig. 3. The $n \times \underline{2}$ phases are characterized by a constant ordering in the $[\bar{1}10]$ direction and a gradual contraction in the [001] direction. The continu-

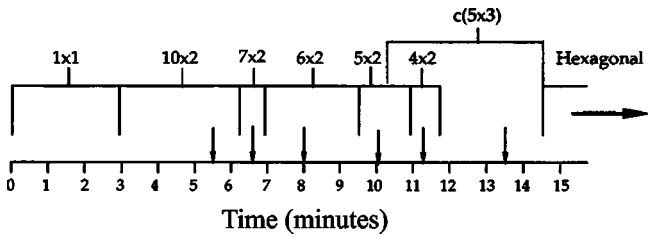

FIG. 3. Phase diagram showing the unit mesh of all the submonolayer structures of Gd on Mo(110). Arrows indicate the points at which the LEED patterns are best formed.

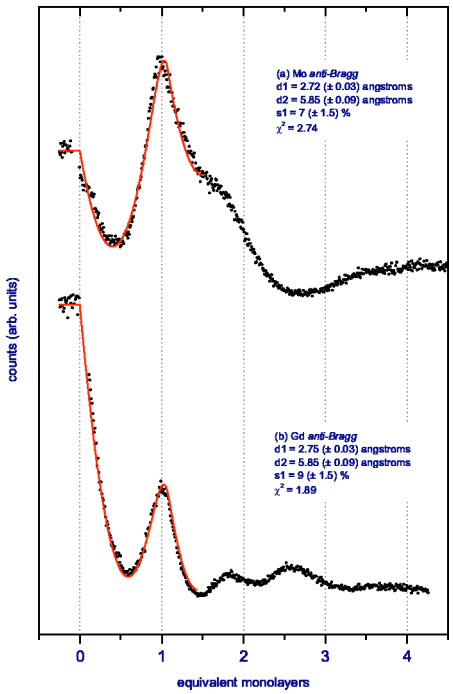

FIG. 4. (Color online) X-ray growth curves (dots) and fits (lines) for Gd deposited on clean Mo(110) at room temperature. Curves have been offset for clarity.

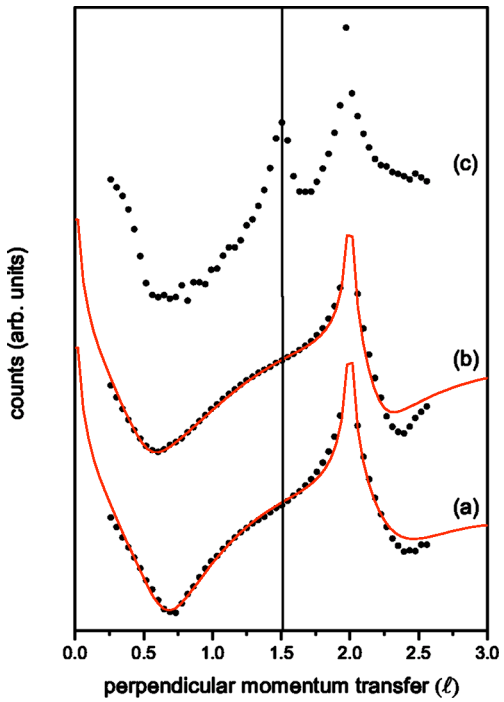

FIG. 5. (Color online) X-ray reflectivity curves for (a) 0.5 ML Gd/Mo(110), (b) 1.0 ML Gd/Mo(110), and (c) 17 ML Gd/Mo(110). Fits to the data (lines) yield values for the layer heights and occupancies, discussed in the text.

ation of this process past the 5×2 structure to the 4×2 overlayer was not observed on W(110).[17] Although on Mo(110) this structure only ever coexists with the $c(5\times3)$ ordering, the 4×2 spots are clear and well defined. The smaller dipole moment for Gd on Mo(110) implies reduced adatom repulsion, which will help to stabilize the more contracted 4×2 structure. Careful measurements of the LEED spot positions reveal a second structural difference between this work and that reported on W(110), namely that the hexagonal monolayer is a Gd(0001) plane contracted by 5.0% compared with 4.4% on the tungsten surface.

Figure 4 shows how the intensity of the specularly scattered x rays changes during the deposition of Gd onto Mo(110) at room temperature. Both curves display an initial peak that can be attributed to the monolayer completion point, followed by weaker features at coverages close to two and three monolayers. This shape is caused by the formation of an initial layer with subsequent growth showing increasing disorder, consistent with the work function change curve shown in Fig. 2. It should be noted that the curve recorded at the Mo anti-Bragg position shows some deviation from the parabolic curve at very low coverage, which is linked to the transition from the random overlayer gas to the formation of ordered structures.

The fits to the curves indicate that the first layer lies 2.74 ± 0.03Å above the Mo surface with the second layer a further 3.11 ± 0.09Å above. If layer separations are calculated assuming the nearest-neighbor distances in the bulk structures (2.73 and 3.57 Å for Mo and Gd respectively), the height for Gd in the highest coordinated adsorption sites is between 2.67 and 2.84 Å, consistent with the fit. The second layer height is expanded in comparison to the (0001) planes of the bulk structure (2.891 Å), most likely due to the increased strain in the first layer. Indeed, within the approximation of a constant cell volume, a layer expansion to 3.08 Å would be expected. The value of s_1 indicates that the second layer is $8.0\pm1.5\%$ full before the first layer is completed, showing that there is some opposition to perfect layer-by-layer growth in this system. The general layerwise growth continues up to approximately 3 monolayers (ML), after which the x-ray intensity remains constant, due to island formation.

Additional spectra were recorded and are shown in Fig. 5 for specific coverages of Gd deposited on Mo(110). These curves show the specular reflectivity as a function of ℓ for Gd deposited to the minimum and maximum points of the first oscillation in the growth curve and for 17 monolayers of Gd. In this case additional correction factors[30] were applied to the data to account for the changing polarization, Lorentz, and area correction factors as the rod scan is measured. The fits to the data were achieved using the rod analysis software developed by Vlieg[31] and include the appropriate number of Gd layers with occupancies and the separation of the layers in the direction perpendicular to the surface.

Figure 5(a) shows the reflectivity data for Gd growth interrupted at the minimum point in Fig. 4. The fit has $\chi^2=2.56$ for a first layer separation of 2.87 ± 0.05 Å and a second layer 3.11 ± 0.05 Å above this. These are close to the values found from the growth curves (2.74 and 3.11 Å, respectively), and we suggest that the expansion in the first layer is due to the improvement in the ordering of one of the reconstructions after deposition was stopped. The occupancies from the fit to the reflectivity correspond to the first

layer containing 55.0±2.5% of a complete Gd monolayer and the top layer 7.0±3.0% of a monolayer, indicating that there is significant second layer incorporation even at this stage of growth.

The data recorded when the growth was stopped at the maximum in the growth curve are shown in Fig. 5(b) together with a fit that yields $\chi^2=1.18$. This fit has a first layer at 2.78±0.03 Å and the second layer at 2.91±0.03 Å above. This is lower than the value identified from the growth curves, which may be due to relaxation of the top layer after removal of the Gd flux. The occupancies of the two layers are 105.0±2.5% and 19.0±3.5% of a complete Gd monolayer, respectively, leading to a total coverage of 1.24 ML. This data indicate that the first layer contains an extra 5% of atoms compared with the RE(0001) plane, supporting the LEED results of a 5% contraction in the initial layer relative to the unrelaxed Gd(0001) planes. At this point in the growth curve there is significant occupation of both the first and second layers.

The data shown in Fig. 5(c) for 17 ML of Gd on Mo(110) have not been fitted, but are included as they show the development of the Bragg peak at $\ell=1.5$ due to the Gd layers. The peak position corresponds to a perpendicular spacing for the Gd layers of 2.97 Å, slightly expanded relative to the theoretical spacing of 2.89 Å.

2. Sm on Mo(110)

A low coordinated monolayer, consisting of divalent Sm with an atomic diameter of 4.29 Å (assuming a 20% expansion relative to trivalent Sm), would have a significant mismatch with the substrate (Mo diameter; 2.73 Å). Sm deposited on Mo(110) has been extensively studied by Stenborg and coauthors,[18,24] who found a range of $n\times 2$ structures and a transition to a near-hexagonal structure approaching a monolayer. One of the most interesting aspects about Sm growth is the dynamic transition from a low coordinated divalent layer to a trivalent buried interface layer as subsequent deposition occurs. Such behavior would affect the transition region between the first and second oscillations in the specularly reflected x-ray curves.

Figure 6 shows how the scattered x-ray intensity varies with time, during the growth of Sm on Mo(110) at room temperature. The upper curve (a) was recorded at the (001) position whilst plots (b) and (c) provide maximum sensitivity to growth in bridge sites of trivalent and divalent Sm, respectively. Figures 6(b) and 6(c) have essentially the same shape, showing an initial oscillation that rises to a peak at one monolayer before decaying to a plateau and remaining at a low level as deposition continues. Figure 6(a) shows an initial parabolic oscillation that rises to a shoulder after a monolayer has been deposited and a smaller oscillation that peaks at close to 2 equivalent monolayers, before decaying to a constant level.

The diffusive model reproduces the shape of each curve shown in Fig. 6. However, beyond ~1.6 equivalent monolayers, there is heavy damping of the oscillations, indicating three-dimensional rough growth after completion of the second layer. This behavior is beyond the scope of the diffusive model and so the fit is limited to the early stages of growth

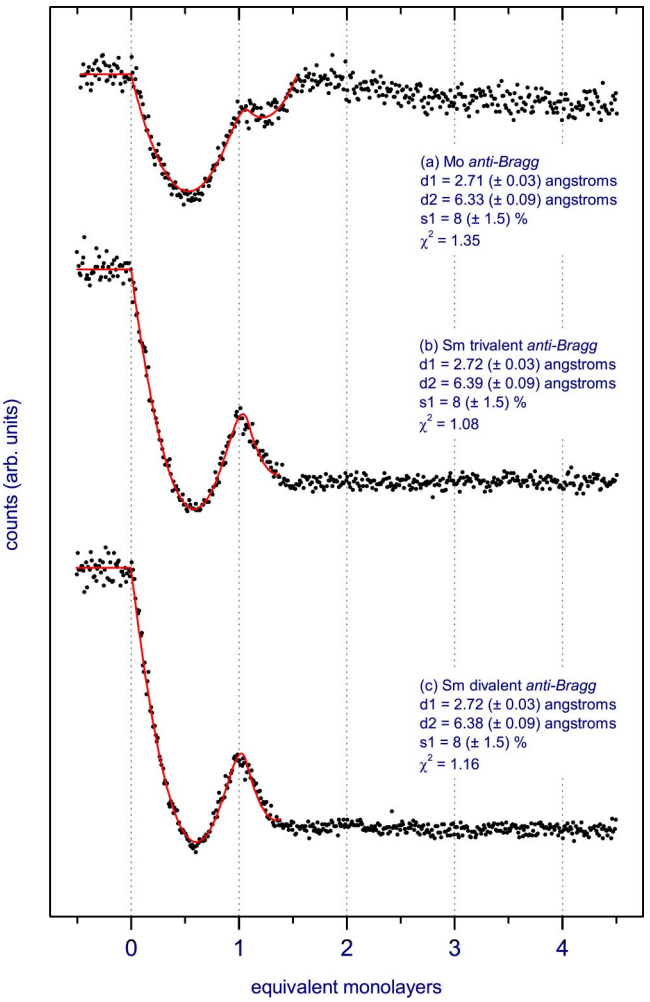

FIG. 6. (Color online) X-ray growth curves (dots) and fits (lines) for Sm deposited on clean Mo(110) at room temperature. Curves have been offset for clarity.

(<1.5 ML). The fitting parameters obtained for the height of the first Sm layer (d_1) shows good agreement between data recorded at different values of ℓ. The average value of $d_1=2.72\pm0.03$ Å is greater than the value of 2.59±0.01 Å found using a simpler growth model,[21] which did not include the diffusive transition region. A hard sphere calculation for a trivalent Sm layer on Mo(110) gives a first layer spacing of 2.70 Å for adsorption into threefold hollow sites, which appears to be in excellent agreement with the value of d_1 obtained from the fits. A Mo(110) surface cannot accommodate a close-packed Sm(0001) monolayer with atoms all in threefold sites. This suggests that the average height of the first layer will be greater than 2.70 Å. The diffusive growth model indexes the height of the adlayers to the Mo bulk layer spacing, and so any relaxation of the outer layers of Mo will appear as a relaxation in the values of d_1 and d_2.

The transition from the completion of the first layer to the start of the second is well described by the fit, with the model predicting that 8.0±1.5% of the second layer is occupied as the first layer is completed. This agrees well with the predictions of Stenborg and Bauer,[24] who found that the initial Sm monolayer has a packing density 4% smaller than a close-

packed Sm(0001) layer. They suggest that second layer atoms are incorporated into the first layer during the initial stages of second layer growth. This idea is essentially identical to having a small period of simultaneous bilayer growth, as predicted by the model.

The values obtained for the second layer heights also show good agreement with an average first to second layer separation of 3.64 ± 0.09 Å. If the second Sm layer is trivalent, and is adsorbed into the threefold hollows of the first trivalent hexagonal layer, then the separation would be 2.95 Å. If the second layer is divalent, then not all of the atoms would sit in threefold sites, due to the larger size of the divalent Sm atom. It has long been accepted that there is a significant increase in radius for divalent Sm in comparison to trivalent Sm atoms[32] due to incomplete mutual electron screening. Recent work by Lundgren *et al.*[7] suggest that the surface layer of Sm is always divalent, with an atom radius 25% larger than that for trivalent atoms. The divalent atoms will fill a variety of adsorption sites across the whole surface, yielding an average layer height somewhere between that expected for the threefold hollow and the on-top positions. It is predicted that the average layer height will be close to the height of atoms adsorbed in twofold bridges sites (3.43 Å for 15% larger divalent atoms and 3.65 Å for 25% larger atoms). We propose that the interlayer spacing derived from the fit in Fig. 6 is due to divalent atoms (25% larger) adsorbed in several bonding sites. A complete divalent layer composed of Sm atoms 25% larger than a trivalent layer would have an atomic density of 5.64×10^{18}atoms m^{-2}, which is 64% of a completely trivalent layer. This would give a second layer completion at 1.64 ML and is likely to be the origin the breakdown of layer-by-layer growth seen at this point.

Growth beyond the first two layers does not show any further oscillations. The deposition of a third layer is complicated by the electronic transition that occurs in the second layer as the Sm atoms gain a coordination greater than 10. The divalent Sm atoms in the open second layer become trivalent as they are enclosed by atoms adsorbed above them, in the third layer. The smaller size of the trivalent state means that the second layer is no longer close packed. Atoms impinging on the surface can therefore be incorporated into the second layer, as well as forming three-dimensional islands.

B. Temperature dependance

The effect of raised substrate temperature on the growth of the two RE's was studied by monitoring the specularly reflected x-ray signal at the (0 0 0.7) position.

1. Gd growth at elevated temperature

Figure. 7 shows how the x-ray intensity varies during deposition of Gd on to a Mo(110) sample held at the temperatures indicated, together with fits to the data using the diffusive model. The general trend is that as the temperature is increased the depth of the first minimum is reduced, and at 140 °C, there is a noticeable shoulder at approximately 0.2 ML. We attribute this feature to the phase change from a random overlayer gas to ordered structures, which is promoted at this higher temperature. As the temperature is raised further to 240 °C, the first minimum continues to get deeper and in this case the breakdown of the model occurs later, indicating that the layerwise growth continues for longer before the onset of islanding. Complex behavior occurs at higher coverage that produces a broad peak, which we interpret as a transition from layerwise growth to island formation due to the high mobility of the Gd adatoms.

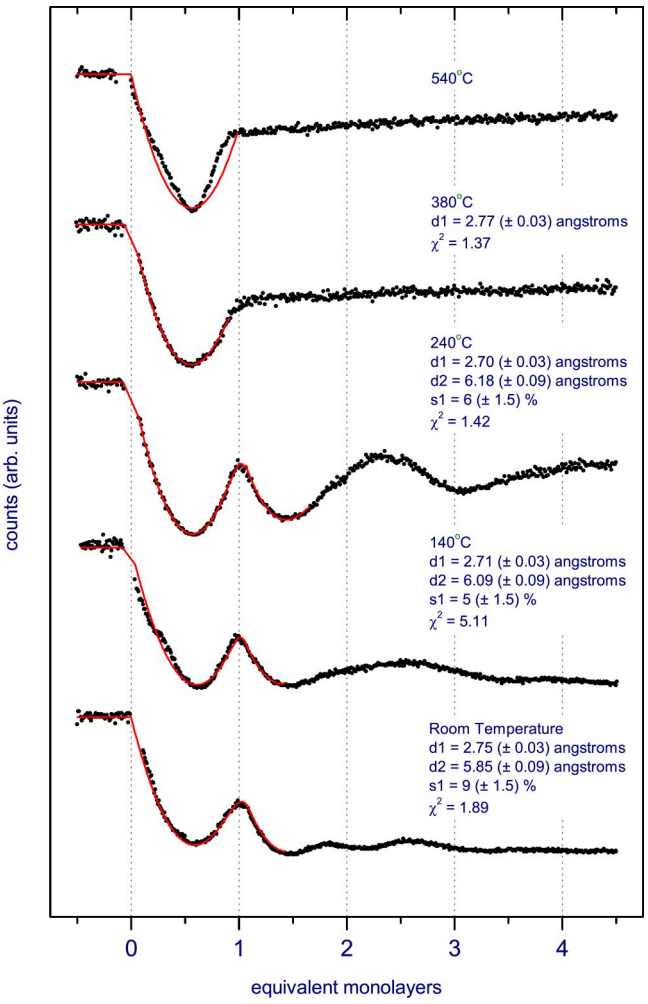

FIG. 7. (Color online) X-ray growth curves (dots) and fits (lines) for Gd deposited on Mo(110) at the temperatures indicated. Curves have been offset for clarity.

Raising the temperature further produces a significant change in the shape of the growth curve. At 380 °C the first parabolic oscillation remains, but all features at higher coverage are absent and the x-ray intensity remains constant due to islanding after completion of the monolayer. The extra mobility of the Gd at the higher temperature allows the adatoms to form islands more readily. At 540 °C the parabolic nature of the first oscillation has been lost and the growth curve can no longer be modeled effectively using the diffusive growth model. The deviation from the model is likely to be due to the formation of Gd islands before the first layer is complete.

The results from the fits to the curves as a function of temperature show some interesting trends. The interfacial

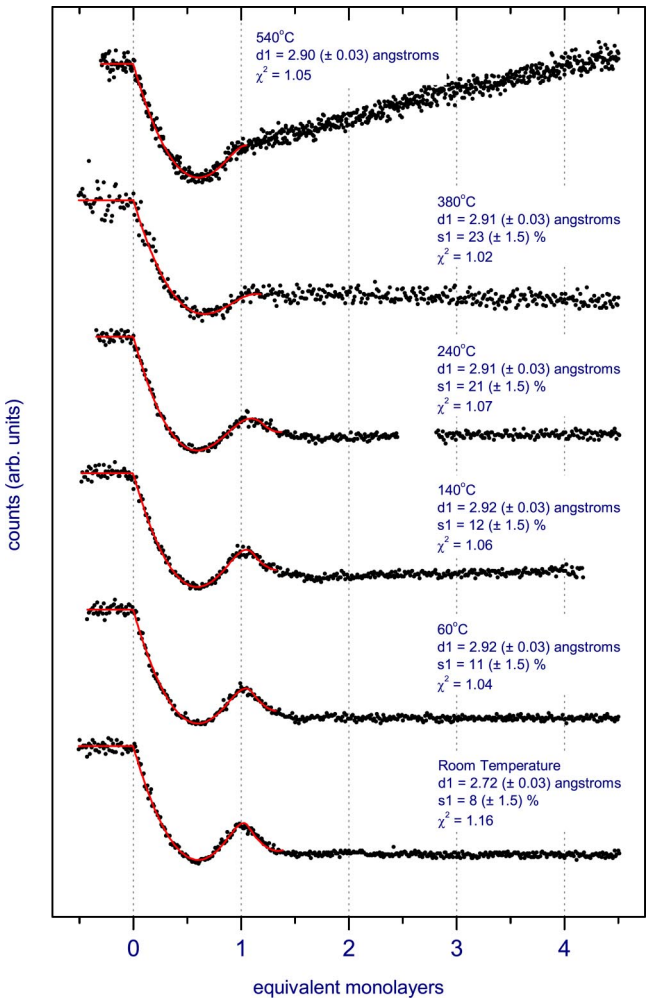

FIG. 8. (Color online) X-ray growth curves (dots) and fits (lines) for Sm deposited on Mo(110) at the temperatures indicated. Curves have been offset for clarity.

layer height remains close to the room-temperature value of 2.75 ± 0.03 Å, indicating that at all temperatures the Gd atoms reside in similar sites, producing no measureable expansion of the layer. The second layer height is, however, significantly expanded at elevated growth temperatures. At room temperature the separation of the two Gd layers is 3.10 ± 0.09 Å whilst at 140 °C it is 3.38 ± 0.09 Å and at 240 °C it is 3.48 ± 0.09 Å. The maximum at the monolayer point in the scattering curve is sharper at the slightly elevated temperatures as shown by the s_1 factor. This reduces from $9.0 \pm 1.5\%$ at room temperature to $5.0 \pm 1.5\%$ at 140 °C, implying that the higher temperature encourages interlayer mass transport and promotes layer by layer growth. This seems to be an optimum temperature for production of the best-quality single monolayer at this deposition rate (0.067 ML/min), as higher growth temperatures result in a Stranski-Krastanov growth mode.

2. Sm growth at elevated temperature

Sm deposition was carried out with the Mo substrate held at several different temperatures. The curves shown in Fig. 8 all share similar features, each having one dominant oscillation in the scattered signal. Subtle changes in the growth mode can be seen as the temperature is increased. The small oscillation, present at the monolayer point in the room-temperature curve, gradually becomes less pronounced as the temperature is increased. At 380 °C the second oscillation can no longer be seen, and the signal plateaus immediately after the first peak. Growth at 540 °C only shows one major oscillation; beyond this the signal slowly increases with further deposition.

The fits to the data show that the first Sm layer becomes expanded as the temperature is increased beyond room temperature. At 60 °C the separation is 7.3% greater than the RT layer height. This does not increase as the temperature is raised further, suggesting there is a critical point somewhere between 25 and 60 °C. The heavy damping of the oscillations after ~1 ML indicates significant islanding that cannot be fitted by the diffusive model. The model breakdown occurs earlier as the growth temperature is increased, so the values of s_1 found at higher temperatures, particularly above 140 °C may not give a clear picture of the actual growth kinetics. Growth at 540 °C clearly shows that surface is becoming smoother due to the increased mobility of the adatoms enabling an annealing process. The mechanism for the expansion of the first layer is likely to be due to the Sm becoming more reactive at higher temperatures, forming hydrides with larger lattice constants from the residual hydrogen present in the UHV chamber.

C. The effects of oxygen exposure

Oxygen has been shown to encourage layerwise growth in several systems including during the growth of Co/Cu spin valves,[33] cobalt on copper(110),[34] nickel on copper(001),[35] and iron on copper(001),[36] a system where CO is also known to improve the growth.[37] In these cases, the oxygen was shown to float to the top of the growing surface, thus acting as a true surfactant. Evidence for this included a nearly invariant oxygen Auger signal during deposition. The proposed surfactant mechanism for Co on Cu(110) is the formation of various oxygen-induced surface reconstructions that are likely to lower the surface energy of the film. The growth of Cr on Cu(001) was found to be unaffected by oxygen predosing,[38] which the authors suggest as being due to the high reactivity between Cr and oxygen atoms. Here we present results showing how oxygen preadsorption affects the growth of Gd and Sm on Mo(110).

1. Gd growth on oxygen-covered Mo(110)

A systematic study was undertaken to establish the role of contaminants on the surface by introducing 0.25 langmuirs of oxygen onto the sample prior to Gd deposition. The curves that resulted for subsequent Gd growth at both the Mo and Gd anti-Bragg positions are shown in Fig. 9. The most obvious difference between these curves and those for Gd deposited on a clean substrate is the increased number of oscillations. In both cases the features are more well defined than for deposition onto the clean substrate and are easily visible to a coverage of greater than 5 ML. This indicates

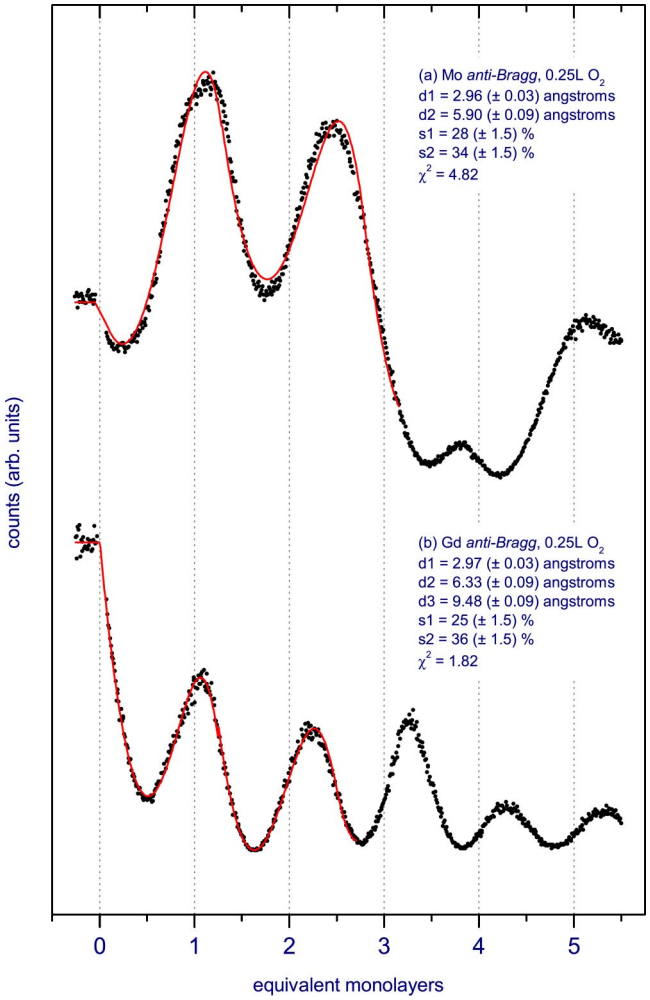

FIG. 9. (Color online) X-ray growth curves (dots) and fits (lines) for Gd deposited at room temperature following exposure of the substrate to the specified amount of oxygen. Curves have been offset for clarity.

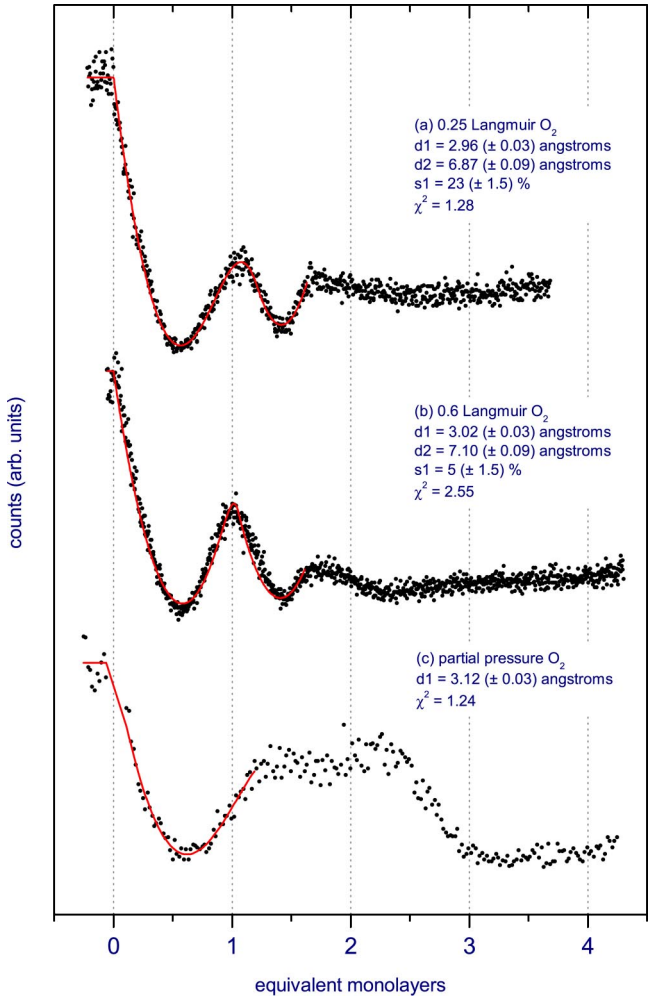

FIG. 10. (Color online) X-ray growth curves (dots) and fits (lines) for Sm deposited at room temperature following exposure of the substrate to the specified amount of oxygen. Curves have been offset for clarity.

that the oxygen is acting as an aid to interlayer mass transport, particularly during growth on top of the initial Gd monolayer.

The fits to the data show an expanded first layer (2.97 ± 0.03 Å) in comparison to growth on clean Mo(110) where the layer separation was 2.74 ± 0.03 Å. This 8% increase is explained by the formation of oxides of gadolinium; GdO in particular has a NaCl type structure and a lattice constant of 5.40 Å, indicating that (111) layers are separated by 3.12 Å, which is 7.9% expanded in comparison to the (0001) planes of gadolinium. Such oxides will form local domains on the surface and act as nucleation centers to enhance the layerwise growth. The fits to the x-ray curve shown in Fig. 9(b) yield a second layer separation from the first of 3.33 ± 0.09 Å and a second to third layer distance of 3.15 ± 0.13 Å. These values are similar to those found for the deposition on the clean substrate and are expanded relative to that expected for Gd (0001) layers. The larger distance in the third layer is evidence of increased strain, which also explains the weaker oscillations observed in layers 4 and 5.

A significant difference is observed for the s_1 factors calculated here and for the clean sample deposition. Whilst more oscillations are seen to exist, the transition between them is less well defined, that is, the cusps between the oscillations are more rounded. This leads to a significant proportion ($\sim$26%) of the second layer being filled before the first is completed, in comparison to the 8% observed for the clean sample. The implication of these results is that although the formation of the GdO complexes encourages layerwise growth there is an extended transition region during which bilayer growth occurs. Fits to the second and third oscillation indicate a similar process for the later growth.

2. Sm growth on oxygen-covered Mo(110)

The results of a study to investigate the role of oxygen as a surfactant in the growth of Sm on Mo(110) are shown in Fig. 10. The upper plot shows the scattered x-ray intensity for the growth of Sm on a Mo(110) surface predosed with 0.25 langmuirs of O_2 (1 langmuir $= 1\ L = 10^{-6}$ Torr S). It has an initial oscillation that a peaks at $\sim$1.1 equivalent monolayers, followed by a smaller oscillation that rises to a peak after $\sim$1.6 equivalent monolayers. If the shape of the curve

is compared to Fig. 6(c) (clean substrate growth), then it is clear that the O_2 dosed sample shows an increased tendency to grow in a layer-by-layer mode. This becomes more apparent when the substrate is predosed with 0.6 langmuirs of oxygen, where the curve has a strong first oscillation, followed by a weaker one peaking at ~1.6 equivalent monolayers. A third, heavily damped oscillation then begins, but upon reaching a minimum never recovers. The lower plot shows the growth of Sm/Mo(110) in a partial pressure of 5×10^{-9} mbar O_2, chosen as this was known to produce the best structures for Co/Cu spin valves.[33] The signal shows just one oscillation peaking after ~1.3 equivalent monolayers followed by a plateau for one equivalent ML, eventually dropping to a low intensity.

The fits to the oxygen-modified growth curves all show an expansion in the first layer spacing. For 0.25 L the expansion is $8.8 \pm 0.5\%$ when compared to clean-film growth. This expansion increases to $11.1 \pm 0.5\%$ for an exposure of 0.6 L and $14.7 \pm 1.5\%$ for Sm grown in a partial pressure of O_2. The height of the second layer is also found to expand by a value of $6.5 \pm 1.5\%$ for a 0.25 L exposure and $12.7 \pm 1.5\%$ for a 0.6 L exposure. This leads to an average first to second layer separation of 4.08 ± 0.09 Å, which shows a $12.7 \pm 2.0\%$ expansion over the nondosed spacing. For growth in a partial pressure of O_2, the fit is limited to the first oscillation, due to the complexity of the growth curve.

The diffusive model predicts that the second layer is $23.0 \pm 1.5\%$ occupied on completion of the first, for an O_2 dose of 0.25 L. This is significantly larger than the value found for the clean Sm deposition, which we explain by rough growth and a limited rate of mass transport in this case. When the O_2 dose is increased to 0.6 L, the model indicates that the second layer is only $5.0 \pm 1.5\%$ occupied when the first is completed. We suggest that this improved growth is not only due to samarium oxides acting as nucleation centers (as with Gd), but also by the suppression of the valence transition and consequent size change in the atoms that occurs during the overgrowth of the first layer.

The role taken by oxygen in the growth of Sm on Mo(110) is somewhat different from the studies outlined at the start of this section. Auger measurements recorded during Sm deposition showed a diminishing oxygen peak, implying that the O_2 is not mobile and is confined to the Mo interface. We propose that the first and second layer expansions are caused by the formation of oxide complexes, on the Mo(110) surface. Layerwise growth is then promoted by SmO island formation. The nucleation of many islands implies a high step density, which encourages interlayer mass transport. The effect of the oxide islands on the mass transport diminishes as they become covered. As with clean-film growth, multilayer island growth dominates when the oxides are completely buried due to the coordination induced valence transition.

IV. SUMMARY

An investigation of the growth and atomic structure of two rare-earth elements, Gd and Sm, deposited on the (110) face of a Mo single crystal has been presented. Surface sensitive *in situ* x-ray scattering has been used to record growth oscillations that have been fitted using a three-level diffusive model. The results reveal the layer structure normal to the surface and also indicate the degree of interlayer mass transport for different experimental conditions. Room-temperature deposition for both elements results in heavily damped oscillations due to layerwise growth that is subsequently replaced by multilayer formation. This is due in part to strain relaxation, although extra roughness is introduced for Sm deposition due to a dynamic transition from a divalent surface state to a trivalent bulk arrangement.

As the temperature of the substrate is raised prior to deposition, the growth becomes slightly modified for both elements. There is an optimum growth temperature of 140 °C for Gd deposited at a rate of 0.067 ML/min, indicating improved interlayer mass transport. Higher deposition temperatures induce earlier multilayer growth, before the first layer is complete. This increased roughness leads to an expanded interlayer distance for subsequent Gd growth. Sm growth shows some changes as the temperature is raised, in particular the first layer is expanded relative to the clean deposition. This is associated with an extended transition region before the first monolayer is completed. As the temperature is further raised, multilayer growth dominates as the mobile Sm atoms cluster together in islands.

The effect of oxygen on the growth was investigated for both elements, by dosing the surface with a known amount of oxygen prior to deposition. In all cases, the presence of oxygen was found to induce more oscillations in the specularly reflected signal, consistent with improved layer-by-layer growth. Although more layers are produced before multilayer formation, the upper layers are found to be significantly occupied before the lower layers are completed. The oxygen is confined to the Mo interface and therefore this is not true surfactant behavior. The results are all consistent with the formation of rare-earth oxide domains at the interface that produce a high density of step edges, which encourages mass transport to the lower layers. The effect produces limited improvement until the oxides are buried. The improvement is less marked for Sm growth on Mo(110), due to the complexity of the growth associated with the changing atom size with valence transition.

[1] D. Weller, S. Alvarado, W. Gudat, K. Schroder, and M. Campagna, Phys. Rev. Lett. **54**, 1555 (1985).
[2] C. Rau and S. Eichner, Phys. Rev. B **34**, 6347 (1986).
[3] T. Kachel, R. Rochow, W. Gudat, R. Jungblut, O. Rader, and C. Carbone, Phys. Rev. B **45**, 7267 (1992).
[4] M. Domke, M. Laubschat, M. Prietsch, T. Mandel, G. Kaindl, and W. Schnieder, Phys. Rev. Lett. **56**, 1287 (1986).
[5] G. Kaindl, C. Laubschat, B. Reihl, R. Pollack, N. Martensson, F.

Holtzberg, and D. Eastman, Phys. Rev. B **26**, 1713 (1982).
[6] B. Johansson, Phys. Rev. B **19**, 6615 (1979).
[7] E. Lundgren *et al.*, Phys. Rev. Lett. **88**, 136102 (2002).
[8] K. Miura, J. Qiu, S. Fujiwara, S. Sakaguchi, and K. Hirao, Appl. Phys. Lett. **80**, 2263 (2002).
[9] M. Lohmeier, W. Huisman, G. ter Horst, P. Zagwijn, E. Vlieg, C. Nicklin, and T. Turner, Phys. Rev. B **54**, 2004 (1996).
[10] M. Lohmeier, W. Huisman, E. Vlieg, A. Nishiyama, C. Nicklin, and T. Turner, Surf. Sci. **345**, 247 (1996).
[11] D. Spence, S. Tear, T. Noakes, and P. Bailey, Phys. Rev. B **61**, 5707 (2000).
[12] D. Spence, T. Noakes, P. Bailey, and S. Tear, Surf. Sci. **512**, 61 (2002).
[13] D. Spence, T. Noakes, P. Bailey, and S. Tear, Phys. Rev. B **62**, 5016 (2000).
[14] Y. Losovyj, I. Yakovkin, S. Barrett, T. Komesu, and P. Dowben, Surf. Sci. **520**, 43 (2002).
[15] N. Moslemzadeh, S. Barrett, and J. Ledieu, Surf. Sci. **521**, L650 (2002).
[16] N. Moslemzadeh, S. Barrett, and J. Ledieu, Phys. Rev. B **66**, 033403 (2002).
[17] J. Kolackiewicz and E. Bauer, Surf. Sci. **175**, 487 (1986).
[18] A. Stenborg, O. Bjorneholm, A. Nilsson, N. Martensson, J. Andersen, and C. Wigren, Phys. Rev. B **40**, 5916 (1989).
[19] A. Stenborg, J. Andersen, O. Bjorneholm, A. Nilsson, and N. Martensson, Phys. Rev. Lett. **63**, 187 (1989).
[20] S. Mozley, C. Nicklin, M. James, P. Steadman, C. Norris, and M. Lohmeier, Surf. Sci. **331-333**, 961 (1995).
[21] C. Nicklin, C. Norris, P. Steadman, J. Taylor, and P. Howes, Physica B **221**, 86 (1996).
[22] E. Weschke, C. Schussler-Langeheine, R. Meier, G. Kaindl, C. Sutter, D. Abernathy, and G. Grubel, Phys. Rev. Lett. **79**, 3954 (1997).
[23] C. Nicklin, J. Taylor, N. Jones, P. Steadman, and C. Norris, J. Synchrotron Radiat. **5**, 890 (1998).
[24] A. Stenborg and E. Bauer, Surf. Sci. **185**, 394 (1987).
[25] M. Farle, K. Baberschke, U. Stetter, A. Aspelmeier, and F. Gerhardter, Phys. Rev. B **47**, 11571 (1993).
[26] M. Farle and K. Baberschke, Phys. Rev. Lett. **58**, 511 (1987).
[27] A. Heys, P. Donovan, A. Petford-Long, and R. Cywinski, J. Magn. Magn. Mater. **131**, 265 (1994).
[28] C. Arcangeli and O. Jepsen, J. Magn. Magn. Mater. **132**, 318 (1994).
[29] R. Nathan and B. Hopkins, J. Phys. E **7**, 851 (1974).
[30] E. Vlieg, J. Appl. Crystallogr. **30**, 532 (1997).
[31] E. Vlieg, J. Appl. Crystallogr. **33**, 401 (2000).
[32] A. Rosengren and B. Johansson, Phys. Rev. B **26**, 3068 (1982).
[33] W. E. Jr., P. Shen, C. Powell, M. Stiles, R. McMichael, J. Judy, K. Takano, and A. Berkowitz, J. Appl. Phys. **82**, 6142 (1997).
[34] W. Ling, Z. Qiu, O. Takeuchi, D. Ogletree, and M. Salmeron, Phys. Rev. B **63**, 024408 (2001).
[35] R. Nunthel *et al.*, Surf. Sci. **531**, 53 (2003).
[36] L. Li, A. Kida, M. Ohnishi, and M. Matsui, Surf. Sci. **493**, 120 (2001).
[37] J. Thomassen, F. May, B. Feldmann, M. Wuttig, and H. Ibach, Phys. Rev. Lett. **69**, 3831 (1992).
[38] M. Ohnishi, L. Li, S. Torii, A. Kida, M. Doi, and M. Matsui, Mater. Trans., JIM **43**, 2143 (2002).